© 2018 IJSRST | Volume 4 | Issue 5 | Print ISSN: 2395-6011 | Online ISSN: 2395-602X
Themed Section: Science and Technology

Vibrational spectral investigations of the FT-IR and FT-Raman spectra and DFT study on 2, 3-pyarazine dicarboxamide

T. Rajalakshmy[1], S. Saravanan[2], D. Henry Raja*[1], V. Balachandran[3]

[1]Department of Physics and Research Centre, Scott Christian College, Nagercoil, India

[2]PG and Research Department of Physics, National College (Autonomous), Tiruchirappalli, India

[3]Centre for Research Department of Physics, A A Government Arts College, Musiri, Tiruchirappalli, India

ABSTRACT

In this work vibrations Spectral analysis on The solid of 2,3-pyarazine dicarboxamide have been investigated both the experimental and theoretical vibration data indicated the presence of variable functional groups with the total of molecule the equilibrium geometry, bonding features, harmonic vibration frequency.IR and Raman intensities have been calculated with the help of density functional theory methods. The assignments of vibration spectra have been carried out the normal co-ordinates analysis following the scaled quantum mechanical force field calculations. The First hyperpolarizability (β_{tot}) of the novel molecules system and related properties (μ, α and Δ_α) are calculated using B-3LYP/6 -31+G (d) and B3LYP/6-311++G (d, p) method on the finite-field approach. The calculated HOMO and LOMO energies show that charger transfer occurs within the molecule. Information about the size shape, charge density distribution and site of chemical reactivity of the molecules has been obtained by mapping elections density is surface With molecular electrostatics potential (MEP).

Keywords: Vibrational spectra, DFT calculations, HOMO-LUMO, DOS Spectrum, MEP Surface

I. INTRODUCTION

The electro negative atom such as halogen attached to the pyarazine in a highly reactive the pyarazine. The 2, 3-pyarazine dicarboxamide is a white crystalline powder with molecular formula ($C_6H_6N_4O_2$).The vibration spectroscopic using DFT methods have reported on methyl phenol. Therefore the present investigation was undertaken study the vibration of FT-IR, FT-Raman spectra of the molecule completely and to identify the vibrations normal modes with grater wave number accuracy. Predication of vibration frequency of polyatomic molecules by quantum chemical calculation has become very popular because of accurate and consistent description of the experimental data.23PDC was investigated by using B3LYP calculation with 6-31+G (d) and 6-311++G (d, p) basis sets.

II. EXPERIMENTAL DETAILS

The sample 23PDC in the white crystal form was provided by the Lancaster Chemical Company (UK) with a purity of greater than 98% and it was used as such without further purification. The FT-Raman spectrum of 23PDC was recorded using 1064 nm line of Nd:YAG laser as excitation wavelength in the region 3500-100 cm^{-1} on a Thermo Electron Corporation model Nexus 670 spectrometer equipped with FT-Raman module accessory. The FT-IR spectrum of 23PDC was recorded in the frequency region 4000-400 cm^{-1} on a Nexus 670 spectrometer

equipped with an MCT detector, a KBr pellet technique.

III. COMPUTATIONAL DETAILS

In order to model the structure and to compare the performance of DFT methods on 23PDC, geometry optimization followed by vibrational frequency calculations were performed at the DFT/B3LYP/6-31+G (d) and B3LYP/6-311++G (d, p) using the GAUSSIAN 09W [1] without any constraint on the geometry. The harmonic vibrational frequencies have been analytically calculated by taking the second-order derivative of energy using the same level of theory. Transformation of force field from Cartesian to symmetry coordinate, scaling, subsequent normal coordinate analysis and calculations of PED, IR and Raman intensities were made on a PC with the version V7.0 of the MOLVIB program written by Sundius [2, 3]. To achieve a close agreement between observed and calculated frequencies, the least-square fit refinement algorithm was used. By combining the results of the GAUSSVIEW [4] with symmetry considerations, along with the available related molecules, vibrational frequency assignments were made with a high degree of accuracy.

Predictions of Raman intensities

The Raman activities (S_R) calculated with the Gaussian 09W program were converted to relative Raman intensities (I_R) using the following relationship derived from the basic theory of Raman scattering [5–7].

$$I_R = \frac{f(\upsilon_0-\upsilon_i)^4 S_R}{\upsilon_i[1-\exp(-hc\upsilon_i/kT)]}$$

where υ_0 is the laser exciting frequency in cm^{-1} (in this work, we have used the excitation wavenumber υ_0=9398.5 cm^{-1}, which corresponds to the wavelength of 1064 nm of a Nd:YAG laser), υ_i is the vibrational wavenumber of the i^{th} normal mode (in cm^{-1}) and S_R is the Raman scattering activity of the normal mode υ_i, f (is the constant equal to 10^{-12}) is a suitably chosen common normalization factor for all peak intensities. h, k, c, and T are Planck constant, Boltzmann constant, speed of light, and temperature in Kelvin, respectively.

FIRST HYPERPOLARIZABILITY

The first hyperpolarizability (β) of this novel molecular system and related properties (α, β and Δβ) of 23PDC were calculated using B3LYP method with 6-31G+ (d) and 6-311++G (d, p) basis sets, based on the finite-field approach. Polarizability and hyperpolarizability characterize the response of a system in an applied electric field [8]. In the presence of an electric field, the energy of a system is a function of the electric field. First hyperpolarizability is a third-rank tensor that can be described by 3x3x3 matrix. The 27 components of the 3D matrix can be reduced to 10 components due to the Kleinman symmetry [9]. It can be given in the lower part of the 3x3x3 matrixes is a tetrahedral. The components of β are defined as the coefficients in the Taylor series expansion of the energy in the external electric field. When the external electric field is weak and homogeneous, this expansion becomes

$$E = E^0 - \frac{\mu_i F_i}{1!} - \frac{\alpha_{ij} F_i F_j}{2!} - \frac{\beta_{ijk} F_i F_j F_k}{3!} - \frac{\gamma_{ijkl} F_i F_j F_k F_l}{4!} + \cdots$$

Where E^0 is the energy of the unperturbed molecules, F_i is the field at the orgin and μ_i, α_{ij}, β_{ijk} and γ_{ijkl} are the components of dipole moment, polarizability and the first hyperpolarizability respectively.

The total static dipole moment is

$$\mu = (\mu_x^2 + \mu_y^2 + \mu_z^2)^{\frac{1}{2}}$$

The isotropic polarizability is

$$\alpha = \frac{\alpha_{xx}+\alpha_{yy}+\alpha_{zz}}{3}$$

The polarizability anisotropy invariant is

$$\Delta\alpha = 2^{-1/2}[(\alpha_{xx}-\alpha_{yy})^2 + (\alpha_{yy}-\alpha_{zz})^2 + (\alpha_{zz}-\alpha_{xx})^2$$

The average hyperpolarizability

$$\beta_{tot} = (\beta_x{}^2 + \beta_y{}^2 + \beta_z{}^2)^{1/2}$$

where

$$\beta_x = \left(\beta_{xxx} + \beta_{xyy} + \beta_{xzz}\right)$$
$$\beta_y = \left(\beta_{yyy} + \beta_{xxy} + \beta_{yzz}\right)$$
$$\beta_z = \left(\beta_{zzz} + \beta_{xxz} + \beta_{yyz}\right)$$

where α_{xx}, α_{yy} and α_{zz} are tensor components of polarizability. β_x, β_y and β_z are tensor components of hyperpolarizability. Since the value of polarizability and hyper polarizability of the GAUSSIAN 09 output are reported in atomic units (a.u.), the calculated values have been converted into electrostatic units (e.s.u.) (1 a.u .=8.639x10^{-33} e.s.u.). The total molecular dipole moment, polarizability and first hyper polarizability are 6.3753 and 6.3292 debye, 1.7560x10^{-30} e.s.u. and 1.7532 x10^{-30}e.s.u. in B3LYP method with6-31+G (d) and 6-311++G (d, p) levels of theory. The dipole moment and mean polarizability and anisotropy polarizability of 23PDC have been recorded in Table 1.

Table 1. The electric dipole moment (μ) (debye), the mean polarizability(α)(e.s.u.), anisotropy polarizability(Δα) (e.s.u.) and first hyperpolarizability(β_{tot}) (e.s.u.) at 2,3-pyrazine dicorboxamide at B3LYP/6-31+G (d) and B3LYP/6-311++G (d, p) methods.

Parameters	B3LYP/6-31+G (d)	B3LYP /6-311++G (d, p)
μ_x	-4.9490	-4.9201
μ_y	1.0737	1.0611
μ_z	3.8730	3.8375
μ	6.37538	6.3292
α_{xx}	-63.3897	-63.4381
α_{xy}	-0.9335	-0.8445
α_{xz}	8.8387	8.7993
α_{yy}	-62.1703	-62.2079
α_{yz}	-5.0521	-4.9814
α_{zz}	-69.6494	-69.6841
A	-65.0698	-65.1100
Δα	109.9973	110.054
β_{xxx}	-33.0954	-33.4929
β_{yyy}	63.3463	62.4176
β_{zzz}	12.3811	12.2773
β_{xyy}	1.1483	1.3841
β_{xxy}	-25.8616	-25.7787
β_{xxz}	21.3325	21.2631
B_{xzz}	5.9194	5.8531
β_{yzz}	-3.0045	-2.6648
β_{yyz}	8.0059	7.8866
β_{xyz}	-12.2425	-12.0801
β_{tot}	1.7560x10^{-30}	1.7532 x10^{-30}

IV. RESULTS AND DISCUSSION

4.1. Molecular geometry

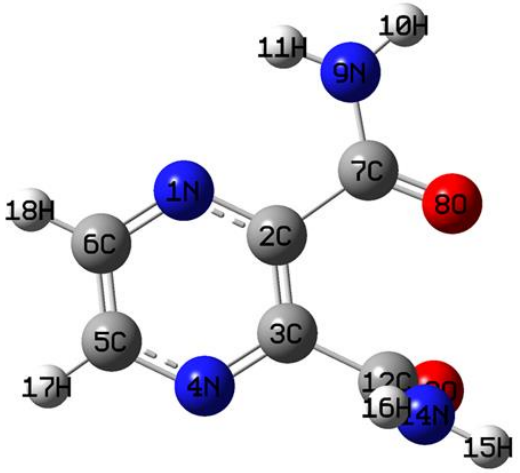

Figure 1. The theoretical geometry structure and atomic numbering scheme of 2,3-pyarazine dicarboxamide

The molecular structure along with numbering of atoms of 23PDC is obtained from Gaussian 09W is as shown in Fig. 1. Optimized geometrical parameters calculated by B3LYP/6-31+G (d) and B3LYP 6-311++G (d, p) basis sets. The experimental geometrical parameters (bond lengths, bond angles) and dihedral angles are listed in Table 2. The optimized bond lengths of C–C lie in the range 1.339–1.334Å and 1.409–1.408Å by B3LYP/6-31+G (d) and B3LYP/6-311++G (d, p) methods, respectively. The calculated bond distances of N_1–C_2, N_1–C_6, C_2–C_3 and C_3–N_4 shows the difference as ~0.021Å, respectively. The electron donating and withdrawing substituent on the benzene ring, the symmetry of the ring is distorted, yielding variation in bond angles at the point of

substitution and at the Para position. The angles at the point of substitutions N_1–C_2–C_3, N_1-C_6-C_5 and C_3-N_4-C_5 are 121.22°, 121.07° and 117.32° in B3LYP method with 6-31+G (d) and B3LYP/6-311++G (d, p) basis sets. Compared with B3LYP method with 6-31+G (d) and 6-311++G (d, p) basis of the bond lengths, bond angles and dihedral angles difference between theoretical approaches have been shown in Figure 2-4, respectively.

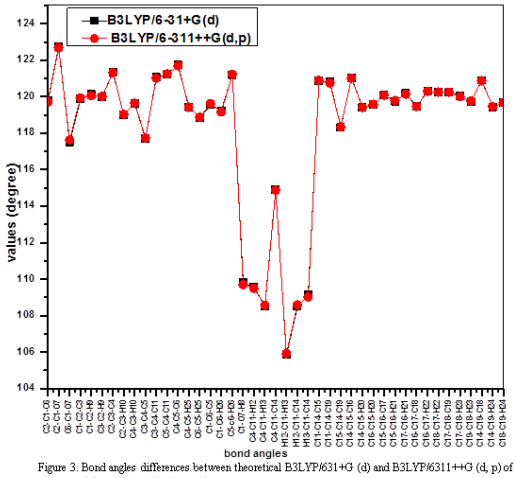

Figure 3. Bond angles differences between theoretical B3LYP/631+G (d) and B3LYP/6311++G (d, p) of 2,3-pyarazine dicarboxamide

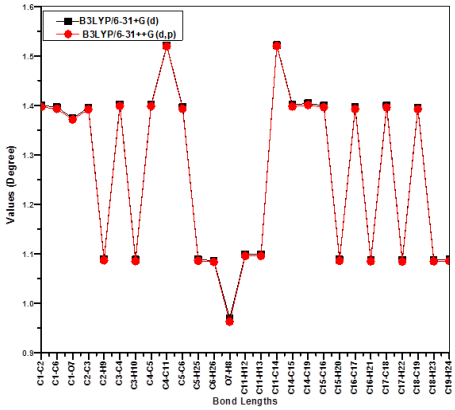

Figure 2. Bond length differences between theoretical B3LYP/631+G (d) and B3LYP/6311++G (d, p) of 2, 3-pyarazine dicarboxamide

Table 2. Optimized geometrical parameters of 2,-3-pyrazine dicorboxamide by B3LYP/6-31+G (d) and B3LYP/6-311++G (d, p) methods.

Bond lengths	Values Å B3LYP		Bond angles	Values degrees B3LYP		dihedral angles	Values degrees B3LYP	
	6-31+G(d)	6-311++G (d, p)		6-31+G (d)	6-311++G (d, p)		6-31+G(d)	6-311++G (d, p)
N_1-C_2	1.339	1.334	C_2-N_1-C_6	117.52	117.65	C_6-N_1-C_2-C_3	2.30	2.75
N_1-C_6	1.335	1.333	N_1-C_2-C_3	121.22	121.07	C_6-N_1-C_2-C_7	175.18	-173.74
C_2-C_3	1.409	1.408	N_1-C_2-C_7	117.54	117.59	C_2-N_1-C_6-C_5	1.33	1.78
C_2-C_7	1.511	1.513	C_3-C_2-C_7	121.19	121.24	C_2-N_1-C_6-H_{18}	179.28	-179.07
C_3-N_4	1.340	1.335	C_2-C_3-N_4	120.85	120.84	N_1-C_2-C_3-N_4	4.32	-5.46
C_3-C_{12}	1.522	1.521	C_2-C_3-C_{12}	123.38	122.75	N_1-C_2-C_3-C_{12}	167.80	166.87
N_4-C_5	1.336	1.335	N_4-C_3-C_{12}	115.34	115.99	C_7-C_2-C_3-N_4	173.07	170.91
C_5-C_6	1.397	1.392	C_3-N_4-C_5	117.32	117.41	C_7-C_2-C_3-C_{12}	14.80	-16.76
C_5-H_{17}	1.088	1.085	N_4-C_5-C_6	121.81	121.68	N_1-C_2-C_7-O_8	163.29	158.58
C_6-H_{18}	1.087	1.085	N_4-C_5-H_{17}	116.94	117.08	N_1-C_2-C_7-N_9	15.88	-20.32
C_7-O_8	1.228	1.220	C_6-C_5-H_{17}	121.25	121.24	C_3-C_2-C_7-O_8	14.20	-17.91
C_7-N_9	1.356	1.355	N_1-C_6-C_5	121.12	121.10	C_3-C_2-C_7-N_9	166.63	163.20
N_9-H_{10}	1.011	1.007	N_1-C_6-H_{18}	117.30	117.40	C_2-C_3-N_4-C_5	2.37	3.21
N_9-H_{11}	1.011	1.008	C_5-C_6-H_{18}	121.57	121.50	C_{12}-C_3-N_4-C_5	170.36	-169.61
C_{12}-O_{13}	1.223	1.216	C_2-C_7-O_8	120.96	120.94	C_2-C_3-C_{12}-O_{13}	78.53	-67.17
C_{12}-N_{14}	1.361	1.356	C_2-C_7-N_9	114.76	114.39	C_2-C_3-C_{12}-N_{14}	107.62	117.90
N_{14}-H_{15}	1.013	1.009	O_8-C_7-N_9	124.28	124.66	N_4-C_3-C_{12}-O_{13}	93.99	105.51
N_{14}-H_{16}	1.011	1.007	C_7-N_9-H_{10}	118.79	118.52	N_4-C_3-C_{12}-N_{14}	79.86	-69.43
			C_7-N_9-H_{11}	120.29	119.79	C_3-N_4-C_5-C_6	1.27	1.32
			H_{10}-N_9-H_{11}	120.24	120.37	C_3-N_4-C_5-H_{17}	179.24	-179.26
			C_3-C_{12}-O_{13}	118.69	119.07	N_4-C_5-C_6-N_1	3.27	-4.00
			C_3-C_{12}-N_{14}	116.54	116.03	N_4-C_5-C_6-H_{18}	177.37	176.88
			O_{13}-C_{12}-N_{14}	124.45	124.69	H_{17}-C_5-C_6-N_1	177.26	176.61
			C_{12}-N_{14}-H_{15}	116.17	117.82	H_{17}-C_5-C_6-H_{18}	2.10	-2.51
			C_{12}-N_{14}-H_{16}	119.43	121.14	C_2-C_7-N_9-H_{10}	176.12	174.56
						C_2-C_7-N_9-H_{11}	5.59	7.59
						O_8-C_7-N_9-H_{10}	3.02	-4.29
						O_8-C_7-N_9-H_{11}	173.55	-171.26
						C_3-C_{12}-N_{14}-H_{15}	172.12	-175.83
						C_3-C_{12}-N_{14}-H_{16}	24.48	-14.04
						O_{13}-C_{12}-N_{14}-H_{15}	14.43	9.55

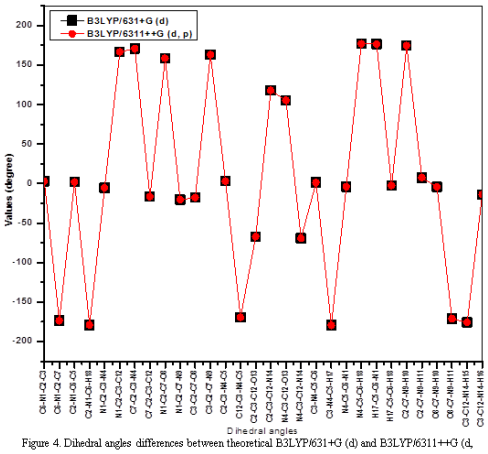

Figure 4. Dihedral angles differences between theoretical B3LYP/631+G (d) and B3LYP/6311++G (d, p) of 2,3-pyarazine dicarboxamide

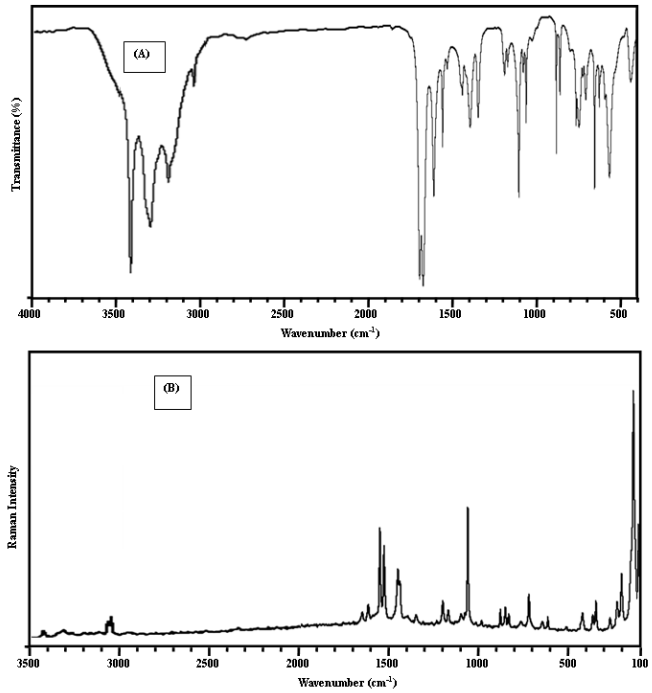

Figure 5. Observed FT-IR (A) and FT-Raman (B) spectra of 2,3-pyarazine dicarboxamide

4.2. Vibrational spectral analysis

In the present study, the spectroscopic signature of 23PDC has been analyzed by the both experimental and theoretical FT-IR and FT-Raman spectra. The Cartesian representation of the theoretical force constant has been computed at the fully optimized geometry by assuming the molecule belongs to C1 point group symmetry. The transformation force field from Cartesian to internal local symmetry coordinates, scaling the subsequent normal coordinate analysis (NCA), calculation of potential energy distributions (PED) results obtained from the MOLVIB program.

A detailed description of vibrational modes can be given by means of normal coordinate analysis. The two distinct scale factors are used to fit the calculated wavenumbers with observed experimental wavenumbers. The observed the FT-IR and FT-Raman spectra of the title molecule shown in Figs.5. The observed FT-IR, FT-Raman wavenumbers and the calculated wavenumbers using DFT/B3LYP method with 6-31+G (d) and 6-311++G (d, P) basis sets along with their relative intensities, probable assignments of the compound are summarized in Table 3.

Amino group vibrations

The fundamental modes involving the amino group are stretching and bending of N–H bonds. For primary amines, N–H stretching vibrations occur in the region 3500–3300 cm^{-1} [10–12]. The amino group has two stretching vibrations namely, asymmetric and symmetric. The asymmetric vibration is higher than symmetric vibration. In the present study, the asymmetric and symmetric vibrations of N–H bond are assigned at 3409 cm^{-1} in FT-IR and 3432 cm^{-1} in FT-Raman, respectively. For in-plane bending vibration (scissoring) observed in the region 1623and1620 cm^{1} [12] and out-of-plane bending vibration observed in the region 1150–900 cm^{-1} [13–16]. In the present compound 23PDC observed in–plane vibrations are found at 1623, 1620, 1546 and 1540cm^{-1} and the out-of-plane bending vibrations are observed at 1196, 1190, 1105 and 1100 cm^{-1}. The theoretically computed values are B3LYP/6-31+G (d) and B3LYP/6-311++G (d, p) methods are approximately coinciding with their observed values is listed in Table 3.

C-H vibrations

For simplicity, modes of vibrations of aromatic compounds are considered as separate C–H or ring C–C vibrations. However, as with any complex molecules, vibrational interactions occur and these labels only indicate the predominant vibration. Substituted benzenes have large number of sensitive

bands, that is, bands whose position is significantly affected by the mass and electronic properties, mesomeric or inductive, of the substituent's [17, 18]. The aromatic structure of C–H stretching vibrations occur the three or four peaks in the region3000–3100 cm^{-1}, these are due to the stretching vibrations of the ring C–H bonds. Since the title compound 23PDC is a tri substituted aromatic system, it has two adjacent and one isolated C–H moieties. Accordingly, in the present study, the C–H stretching vibrations observed at 3182 cm^{-1}. The theoretically computed values for C–H stretching vibrations at B3LYP/6-31+G (d) and B3LYP/6-311++G (d, p) methods are correlated with absorbed values. All the C–H vibrations are in line with the literature values. The C–H in-plane and out-of-plane bending vibrations generally lies in the range 1000–1300 $cm^{-1}$and 1000–675 cm^{-1} [19, 20] their characteristic region. The FT-IR bands at 872cm^{-1} are assigned to C-H to in-plane bending vibration of 23PDC. The C–H out-of-plane bending vibrations of the 23PDC are well identified at 1278, 1148 cm^{-1} in FT-Raman and 956 cm^{-1} in FT-IR. This drastic change in the usual behaviour of aromatic C–H stretching in this compound may be due to the presence of strong N–H stretching vibrations.

Ring *vibrations*

The ring C=C and C–C stretching vibrations, known as semicircle stretching usually occurs in the region 1625–1400 cm^{-1} [22].The C=C stretching vibrations of the present compound are strongly observed at 1664, 1514 and 1493 cm^{-1} in FT-Raman and 1622 cm^{-1} in FT-IR. These assignments are in line with the literature [23]. The bands for C–C stretching vibrations are observed at 1081 cm^{-1} in FT-Raman and 1564, 1523 and 1075 cm^{-1} in FT-IR. All the bands lie in the expected range except the last band when compared to the literature values. Several ring modes were affected by the substitution to the aromatic ring of the title compound. This view shows the domination character of amine group. The C-N-C in-plane bending vibrations observed at 724 cm^{-1} and computed values 654 and 597 cm^{-1}. The out-of-plane bending vibrations at 428 and 336 cm^{-1} assigned only in FT-Raman and computed values are 411 and 375 cm^{-1}. Except last two values of out-of-plane bending vibrations, these assignments are in good agreement with the literature [24, 25]. The theoretically computed value B3LYP/6-31+G (d) and B3LYP/6-311++G (d, p) basis sets values are good agreement with observed values.

C–N vibrations

The C–N stretching frequency is rather difficult task since there are problems in identifying these frequencies from other vibrations [26]. Silverstein [27] assigned C–N stretching absorption in the region 1386 and 1266 cm^{-1} for aromatic amines. In the present work, the band observed at 1330cm^{-1} in FT-IR and 1321 cm^{-1} in FT-Raman spectrum has been assigned to stretching vibration between carbon and nitrogen atoms which is in line with the literature [28–30]. In present case, the C–N in-plane bending and C–N out-of-plane bending vibration have been assigned at 362,350, and 268 cm^{-1} in B3LYP/6-31+G (d) and B3LYP/6-311++G (d, p), respectively. These assignments are in line with the literature values [31]. The reminder of the observed and calculated frequencies accounted in Table 3. This implies that the C–N vibrations are not much influenced by other substitutions in the ring and also this vibration not influenced by amine.

C=O vibrations

Carbonyl group vibrations in ketones are the best characteristic bands in vibrational spectra, and for this reason, such bands have been the subject of extensive studies [32, 33]. The intensity of these bands can increase because of conjugation, therefore, leads to the intensification of the Raman lines as well as the increased infrared band intensities. The carbonyl stretching vibrations in ketones are expected in the region 1715 and 1680 cm^{-1}. In this case, a very strong band at 1674 cm^{-1} in FT-IR and strong band at 1671

cm^{-1} in FT-Raman spectra are assigned as C=O in-plane bending vibration is found at 724 and 726 cm^{-1} in FT-IR and FT-Raman values is well agreement with calculated values 765 and 762 cm^{1} at B3LYP method with 6-31+G (d) and 6-311++G (d, p) of basis sets. The out-of-plane bending vibration of 23PDC, theoretically calculated at 210and 207 cm^{-1} is excellent agreement with the literature value [34].

Table 3. Vibrational assignments of FT-IR and FT-Raman peaks along the theoretically computed wavenumbers, IR intensity (I_{IR}) and Raman intensity (I_{Raman}) and the percentage of potential energy distribution.

S.No	Observed wave number (cm^{-1})		Calculated wave number (cm^{-1})								Assignments with % of PED
	FT-IR	FT-Raman	B3LYP/6-31+G (d)				B3LYP/6-311++G (d, p)				
			Un scaled	Scaled	I_{IR}	I_{Raman}	Un scaled	Scaled	I_{IR}	I_{Raman}	
1		3432	3712	3440	75.9	52.895	3717	3441	457.2	259.55	NH_2 ass(97)
2	3409		3685	3413	34.0	58.021	3716	3410	256.2	197.70	NH_2 ass(97)
3		3316	3582	3322	54.2	155.755	3586	3320	199.0	141.61	NH_2 ss(98)
4	3285	3277	3565	3293	48.7	166.948	3583	3290	170.4	78.21	NH_2 ss(99)
5		3182	3205	3193	33.6	266.695	3178	3196	162.2	55.57	υCH(91)
6		3062	3188	3060	0.8	83.053	3161	3062	98.4	53.25	υCH(96)
7			1775	1700	342.9	35.086	1766	1695	84.2	44.25	υC=O(98)
8			1766	1680	353.9	29.303	1759	1678	83.0	41.24	υC=O(97)
9	1620	1623	1654	1626	85.9	7.027	1624	1619	79.6	38.96	NH_2 sciss(69)
10		1564	1621	1568	169.9	18.044	1601	1561	70.2	27.29	υCC(66)
11	1546	1540	1599	1548	7.7	29.140	1590	1541	59.7	24.99	NH_2 sciss(68)
12		1523	1591	1532	4.3	44.055	1577	1420	54.7	19.90	υCC(63)
13	1446	1450	1485	1453	15.4	0.974	1475	1447	53.4	18.16	υCCN(62)
14	1395		1456	1399	9.7	30.584	1445	1392	53.0	14.38	υCCN(63)
15		1350	1399	1357	185.9	8.622	1383	1352	46.5	13.30	υCCN(61)
16	1330	1321	1363	1327	90.8	10.012	1349	1352	45.7	11.82	υCN(77)
17		1256	1261	1358	4.6	0.776	1253	1323	32.9	8.53	υCN(76)
18		1230	1246	1234	15.1	3.329	1230	1357	29.1	7.29	υCCN(60)
19	1190	1196	1214	1198	39.6	17.400	1203	1228	25.5	7.21	NH_2 wag(61)
20	1105	1100	1124	1107	15.8	3.602	1119	1193	23.1	6.86	NH_2 wag(66)
21	1081		1114	1088	34.7	6.077	1100	1103	20.5	4.16	υCC(68)
22		1075	1094	1079	18.0	0.679	1089	1077	20.2	3.45	υCC(67)
23	1058		1089	1061	4.7	37.832	1086	1060	19.6	3.19	υCC(67),βCH(7)
24		956	988	960	0.1	0.332	988	954	17.3	3.15	βCH(60),υCC(67)
25	872		884	877	15.7	0.365	884	870	16.1	3.13	βCH(55), υCC(67)
26	765	762	790	768	6.1	3.132	793	760	12.1	1.98	βC=O(52)
27		748	759	753	3.2	1.155	768	750	10.9	1.59	βCCC(50)
28	720	722	734	726	30.8	4.965	746	720	10.9	1.57	βC=O(53)
29	706		721	711	5.9	0.564	730	707	10.6	1.54	βCCC(47)
30	651	660	677	666	12.0	14.218	780	657	9.0	1.54	βCCC(53)
31			628	614	25.6	1.944	629	612	8.4	1.51	βCCC(52)
32			619	609	9.5	1.055	620	605	5.8	1.38	γCCC(60)
33	581		614	590	1.1	0.399	604	580	5.7	1.26	NH_2 rock(40)
34	558		597	563	2.1	1.145	594	560	5.4	1.18	NH_2 rock(43)
35		512	539	516	42.7	0.872	543	519	5.1	1.00	γCCN(42)
36			503	489	60.4	0.963	507	491	4.6	0.94	γCCN(40)
37			441	433	72.2	0.272	439	431	4.6	0.88	γCCN(43)
38		425	433	422	126.7	0.740	436	420	3.9	0.81	γCCN(42)
39		362	375	367	4.1	3.326	380	363	3.8	0.71	βCN(51)
40		350	356	354	13.8	0.454	352	350	3.8	0.70	βCN(53)

41			327	319	171.0	1.299	319	317	3.5	0.67	NH_2 twis(43)
42		268	296	272	20.5	2.221	300	265	3.5	0.66	γCN(47)
43		237	242	243	13.0	1.764	244	239	3.3	0.61	γCN(43)
44		143	156	147	10.2	3.245	162	142	2.2	0.57	NH_2 twis(40)
45		112	142	117	6.7	0.710	144	113	2.0	0.49	γCCC(43)
46			99	93	2.2	1.510	100	92	1.2	0.35	γCCC(42)
47			67	66	12.8	1.369	74	64	0.3	0.34	γCCC(41)
48			22	20	13.7	3.909	11	10	0.2	0.30	γCCC(46)

ass – asym stretching, ss – sym stretching, ipb – in-plane-bending, opb – out-of-plane bending, sb – symd bending, ipr – in-plane rocking, opr – out-of-plane rocking, sciss – scissoring, rock – rocking, wagg – wagging, twist – twisting.

Assignments: ν - stretching, β - in-plane bending, γ- out-of-plane bending.

4.3. Mulliken atomic charges

The Mulliken atomic charges calculation has an important role in the application of quantum mechanical calculations to molecular system [35] because of atomic charges effect dipole moment, molecular polarizability, electronic structure and more a lot of properties of molecular systems. Mulliken atomic charges calculated at the DFT/B3LYP/6-31+G (d) and /6-31++G (d) methods is presented in Table 4. It is worthy to mention that H_{15} atom is more acidic due to more positive charge. The Mulliken atomic charges of the phenol group hydrogen atom N_9 are higher than the aromatic group and methyl group hydrogen. It denotes that the phenol group hydrogen atoms are more acidic than the aromatic and methyl group hydrogen atoms, however that the high value 0.422193e and 0.3031e for H_{15} in B3LYP and methods with 6-31+G (d) ,6-311++G (d, p) basis sets. The N_9 atom exhibit high negative charge is $-0.8546e^-$ for B3LYP/6-31+G (d) and $-0.3979e^-$ for 6-311++G (d, p) methods. The results can however better represent in graphical form as given Figure 6, respectively.

Table 4. Mulliken's population analysis of 2,3-pyrazine dicorboxamide at B3LYP/6-31+G (d) and B3LYP/6-311++G (d, p) methods.

S. No.	Atom No.	Mulliken's Atomic charges	
		B3LYP/6-31+G (d)	B3LYP/6-311++G (d, p)
1	N_1	-0.2685	-0.0696
2	C_2	0.0206	0.6007
3	C_3	0.2956	-0.3116
4	N_4	-0.1873	0.0623
5	C_5	-0.0749	-0.0102
6	C_6	0.1013	0.1156
7	C_7	0.2490	-0.2361
8	O_8	-0.4971	-0.2818
9	N_9	-0.8546	-0.3979
10	H_{10}	0.4321	0.3270
11	H_{11}	0.4216	0.2705
12	C_{12}	0.3347	-0.5154
13	O_{13}	-0.4362	-0.2705
14	N_{14}	-0.7569	-0.2592
15	H_{15}	0.4222	0.3031
16	H_{16}	0.3920	0.2499
17	H_{17}	0.2006	0.2153
18	H_{18}	0.2058	0.2078

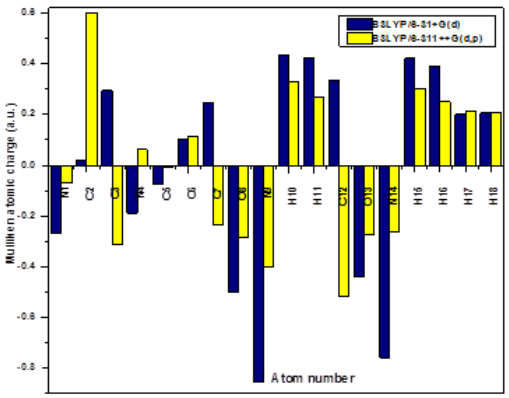

Figure 6. Mulliken population analysis chart of 2, 3-pyarazine dicarboxamide at B3LYP/631+G (d) and B3LYP/6311++G (d, p) methods.

4.4. Frontier molecular orbitals

The most important frontier molecular orbital's (FMOs) such as highest occupied molecular orbital (HOMO) and lowest unoccupied molecular orbital (LUMO) plays a crucial part in the chemical stability of the molecule [36]. The HOMO represents the ability to obtain an electron. The frontier orbital gap helps to characterize the chemical reactivity, kinetic stability, optical polarizability and chemical hardness-softness of a molecule [37]. A molecule with a small frontier orbital gap is more polarizable and is generally associated with a high chemical reactivity, low kinetic stability and is also termed as soft molecule [38]. The low values of frontier orbital gap in 23PDC make it more reactive and less stable. The HOMO is the orbital that primarily acts as the electron donor and the LUMO is the orbital that primarily acts as the electron acceptor. The 3D plot of the frontier orbital's HOMO and LUMO, and their orbital energy gaps are calculated by B3LYP method with 6-31+G (d) and 6-311++G (d, p) basis sets for 23PDC molecule are shown in Fig. 7. The positive phase is red and the negative one is green (for interpretation of the references to color in this text, the reader is referred to the web version of the article). Many organic molecules, containing conjugated π-electrons characterized by large values of molecular first hyperpolarizabilities were analyzed by means of vibrational spectroscopy [39]

Generally, the energy gap between the HOMO and LUMO decreases, it is easier for the electrons of the HOMO to be excited. The energy of HOMO, to easier it is for LUMO to accept electrons when the energy of LUMO is low. The energy gap values of HOMO to LUMO levels are computed to be ΔE= 4.132 and 4.101eV for B3LYP methods with 6-31G+ (d) and 6-311++G (d, p) basis sets, respectively. In the case of 23PDC, the smallest energy gap of values are identified between the HOMO and LUMO with the help of B3LYP/6-31+G (d) and B3LYP/6-311++G (d, p) methods in Table 5. Pauling introduced the concept of electronegativity as the power of an atom in a compound to attract electrons to it. Hardness (η), chemical potential (μ), electronegativity (χ), global softness (σ), ionization potential (I), electron affinity (A) and global electrophilicity (ω) are defined follows:

$$\eta = \frac{1}{2}\left(\frac{\partial^2 E}{\partial N^2}\right)_{V(r)} = \frac{1}{2}\left(\frac{\partial \mu}{\partial N}\right)_{V(r)}$$

$$\mu = \left(\frac{\partial E}{\partial N}\right)_{V(r)}$$

$$\chi = -\mu = -\left(\frac{\partial E}{\partial N}\right)_{V(r)}$$

where E is the total energy, N is the number of electrons of the chemical species and η is the chemical potential and V(r) is the external potential, which is identified as the negative of the electronegativity (χ) as defined by Iczkowski and Margrave [40]. According to Koopman's theorem [41], the entries of the HOMO and the LUMO orbital's of the molecule are related to the ionization potential (I) and the electron affinity (A), respectively, by the following relations:

$$I = -E_{HOMO}$$

$$A = -E_{LUMO}$$

where I and A are ionization potential and electron affinity of the compound respectively. Electron affinity refers to the capability of ligand to accept precisely one electron from a donor. However, in many kinds of bonding viz covalent hydrogen bonding, partial charge transfer takes place). Absolute electronegativity (χ) and hardness (η) of the molecule are given by [42], respectively. Softness (σ) is a property of compound that measures the extent of chemical reactivity. It is the reciprocal of hardness.

$$\chi = (1 + A)/2$$

$$\eta = (1 - A)/2$$

$$\sigma = \frac{1}{\eta}$$

Parr et al. [43] have defined global electrophilic power of the compound as electrophilicity index (ω) in terms of chemical potential and hardness as follows.

$$\omega = \left(\frac{\mu^2}{2\eta}\right)$$

All the calculated values of quantum chemical parameters of the molecules in B3LYP method with 6-31+G (d) and 6-311++G (d, p) basis sets are presented in Table 5.

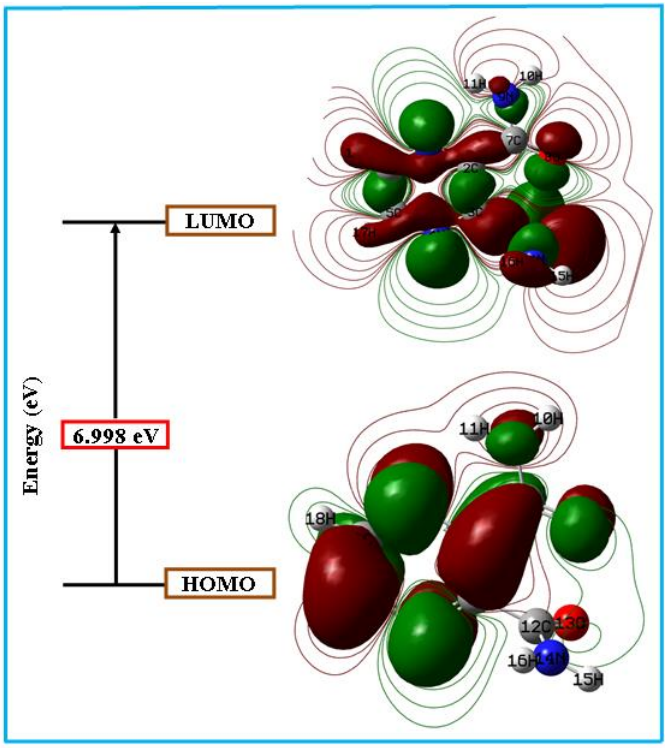

Figure 7. The atomic orbital composition of the frontier molecular orbital for 2,3-pyarazine dicarboxamide

Table 5. Comparison of HOMO and LUMO energy gap and related molecular properties of 2,3-pyrazine dicorboxamide at B3LYP/6-31+G (d) and B3LYP/6-311++G (d, p) methods.

Molecular properties	Energy (a.u)	Energy gap (eV)	Ionization potential (*I*)	Electron affinity (*A*)	Global Hardness (η)	Electro negativity (χ)	Global softness (υ)	Chemical potential (μ)	Global Electrophilicity (ω)
B3LYP/6-31+G(d)									
HOMO	-0.2571	4.1328	6.998	2.865	2.066	4.932	358.32	4.932	33.9422
LUMO	-0.1053								
B3LYP /6-311++G(d, p)									
HOMO	-0.2588	4.101	7.044	2.942	2.050	4.993	361.04	4.993	34.529
LUMO	-0.1081								

4.5. Molecular electrostatic potential (MEP)

Molecular electrostatic potential (MEP) at a point in the space around a molecule gives an indication of the net electrostatic effect produced at that point by the total charge distribution (electron + nuclei) of the molecule and correlates with dipole moments, electro negativity, partial charges and chemical reactivity of the molecule. It provides a visual method to understand the relative polarity of the molecule. V(r), at a given point r(x, y, z) in the vicinity of a compound, is defined in terms of the interaction energy between the electrical charge generated from the compound electrons and nuclei and positive test charge (a proton) located at r. Unlike, many of the other quantities used at present, and earlier as indices of reactivity V(r) is a real physical property that can be determined experimentally by diffraction or by computational methods. For the systems studied the molecular electrostatic potential values were calculated as described previously, using the equation [43].

$$V(r) = \sum \frac{Z_A}{|R_A - r|} - \int \frac{\rho(r')}{|r' - r|} dr$$

Where the summation runs over all the nuclei A in the compound and polarization and reorganization effects are neglected. Z_A is the charge of the nucleus A, located at R_A and $\rho(r')$ is the electron density function of the molecule.An electron density is surface mapped with electrostatic potential surface depicts the size, shape, charge density and site of chemical reactivity of the molecule, the electron density isosurface being 0.002a.u. The different values of the electrostatic potential represented by different colors; red represents the regions of the most negative electrostatic potential, blue represents the regions of the most positive electrostatic potential and green represents the region of zero potential. Potential increases in the order red < orange < yellow < green < blue. Such mapped electrostatic potential surfaces have been plotted for title molecule. Fig.8 shows the plot of molecular electrostatic potential surface of 23PDC along with the computationally derived electrostatic potential and electrostatic point charges on its individual atoms. It is clear from the figure that the atoms N_1, N_{14}, N_9, $C_2$and O_{13} holds significant electronegative charges and the atoms C_2, C_5, H_{10}, H_{10} and C_{12} holds significant positive charges. The halogen group in the molecule is influenced by the stereo structure and the charge density distribution. These sites show regions of most negative electrostatic potential and high activity of the halogen groups. The fitting point charge to the electrostatic potential indicates that the atom F_{12}, And F_{13} are the most electronegative (-1.01244 and -0.5362) atom for 23PDC molecule. As we have mentioned earlier, the electrostatic potential has been used primarily for predicting sites and relative reactivity's towards electrophilic attack, and in studies of biological recognition and hydrogen bonding interactions [45, 46].

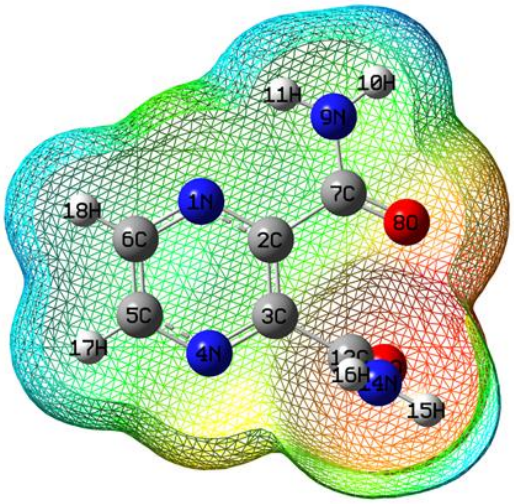

Figure 8. Calculated 3D molecular electrostatic potential contour map of 2,3-pyarazine dicarboxamide

V. CONCLUSION

The present work for the proper vibrational frequency assignments for the compound of 23PDC from the FT-IR and FT-Raman spectra have been recorded for the first time. The equilibrium geometries, harmonic vibrational frequencies, IR intensities and Raman intensities of the title compound were determined and analyzed by both at DFT/B3LYP level of theory utilizing 6-31+G (d) and 6-311++G (d, p) basis sets. We have carried out density functional theory calculations on the structure, vibrational spectra, electric dipole moment, polarizability and the hyperpolarizability, HOMO–LUMO analyses of the compound. On the basis of agreement between the calculated and experimental results assignments of all the fundamental vibrational modes of 23PDC are examined and proposed in this investigation. The electric dipole moments and first hyperpolarizability of the compound studied have been calculated by DFT/B3LY method with 6-31+G (d) and 6-311++G (d, p) basis sets. The DFT calculated non-zero μ value of this ligand shows that the 23PDC compound might have microscopic first hyperpolarizability with non-zero values obtained by the numerical second derivatives of the electric dipole moment according to the applied field strength. The lowering of HOMO–LUMO energy gap explains the eventual

charge transfer interactions takes place within the molecule. The MEP map shows the negative potential sites are oxygen atoms O_8 and O_{13} as well as the positive potential sites on the molecules.

VI. REFERENCES

[1]. M.J. Frisch, et al., GAUSSIAN 09, Revision A. 9, Gaussian, INC, Pittsburgh, 2009.

[2]. T. Sundius, J. Mol. Struct. 218, 1990, 321-326; MOLVIB: A Program for Harmonic Force field calculations.QCPE Program No. 807, 2002.

[3]. T. Sundius, Vib. Spectrosc. 29, 2002, 89-95.

[4]. A. Frisch, A.B. Nelson, A.J. Holder, GAUSSVIEW User Manual, Gaussian Inc., Pittsburgh, CT, 2009.

[5]. P.L. Polavarapu, J. Phys. Chem. 94, 1990, 8106-8112.

[6]. G. Keresztury, BT Raman spectroscopy. Theory, in: J.M. Chalmers, P.R. Griffiths (Eds.), Handbook of Vibrational Spectroscopy, vol. 1, John Wiley & Sons Ltd., 2002, p. 71-87.

[7]. G. Keresztury, S. Holly, J. Varga, G. Besenyei, A.Y. Wang, J.R. Durig, Spectrochim. Acta A 49, 1993, 2007-2017.

[8]. V. Krishnakumar, G. Keresztury, T. Sundius, R. Ramasamy, J. Mol. Struct. 702, 2004, 9-21.

[9]. A. Kleinman, J. Phys. Rev. 126, 1962, 1977-1979.

[10]. Y. Wang, S. Saebo, C.V. Pittman, J. Mol. Struct. (Theochem.) 281, 1993, 91-98.

[11]. A. Altun, K. Golcuk, M. Kumru, J. Mol. Struct. (Theochem) 637, 2003, 155-169.

[12]. N. Puviarasan, V. Arjunan, S. Mohan, Turkey J. Chem. 26, 2002, 323-334.

[13]. M.S. Refat, S.A. El-Korashy, A.S. Ahmed, Spectrochim. Acta A 70, 2008, 840-849.

[14]. H.F. Hameka, J.O. Jensen, J. Mol. Struct. (Theochem.), 1996, 325-330.

[15]. N. Vijayan, R.R. Babu, R. Gopalakrishnan, P. Ramasamy, M. Ichimura, M. Palanichamy, J. Crystal Growth, 2005, 564-569.

[16]. G. Varsanyi, Vibrational Spectra of Benzene Derivatives, Academic Press, New York, 1969.

[17]. B. Revathi, V. Balachandran, Elixir-Vib.Spectrosc. 48, 2012, 9467-9470.

[18]. M. Ramalingam. S. Periandy, B. Narayanan, S. Mohan, Spectrochim. Acta A 76 , 2010, 84-92.

[19]. G. Eazhilarasi, R. Nagalakshmi, V. Krishnakumar, Spectrochim. Acta A 71, 2008, 502-507.

[20]. V. Krishnakumar, N. Prabhavathi, Spectrochim. Acta A 71, 2008, 449- 457.

[21]. A. Altun, K. Golcuk, M. Kumru, J. Mol. Struct. (Theochem.) 637, 2003, 155-169.

[22]. N.P. Singh, R.A. Yadav, Indian J. Phy. B 75 (4), 2001, 347-355.

[23]. R.L. Peesole, L.D. Shield, I.C. Mcwillam, Modern Methods of Chem. Analysis, Wiley, New York, 1976.

[24]. A.R. Prabakaran, S. Mohan, Indian J. Phy. B 63, 1989, 468-473.

[25]. V. Krishnakumar, V. Balachandran, Spectrochim. Acta A 61, 2005, 1811- 1819.

[26]. N. Sundaraganesan, H. Saleem, S.Mohan, M. Ramalingam, V. Sethuraman, Spectrochim.Acta A 62, 2005, 740-751.

[27]. M. Silverstein, G.C. Basseler, C. Morill, Spectrometric Identification of Organic Compound, Wiley, New York, 1981.

[28]. L.J. Bellamy, R.L. Williams, Spectrochim. Acta A 9, 1957, 341-345.

[29]. V. Arjunan, S. Mohan, Spectrochim. Acta A 72, 2009, 436-444.

[30]. J. Swaminathan, M. Ramalingam, N. Sundaraganesan, Spectrochim. Acta A 71, 2009, 1776-1782.

[31]. G.Socrates, IR and Raman characteristics Group Frequencies Tables and Charts, 3rd Ed., Wiley, Chechester, 2001, pp. 107.

[32]. G. Socrates, Infrared Characteristic Group Frequencies, John Wiley & Sons,Interscience Publication, New York, Brisbane, Toronto 1980

[33]. B. Smith, Infrared Spectral Interpretation, A Systematic Approach, CRC Press, Washington, DC, 1999.

[34]. A.J. Abkowicz-Bienko, Z. Latajka, D.C. Bienko, D. Michalska, Chem. Phys. 250, 1999,

[35]. N. Sundaraganesan, H. Saleem, S.Mohan, M. Ramalingam, V. Sethuraman, Spectrochim.Acta A 62, 2005, 740-751..

[36]. B. Kosar, C. Albayrak, Spectrochim. Acta A 78, 2011, 160-167.

[37]. P. Senthil Kumar, K. Vasudevan, A. Prakasam, M. Geetha, P.M. Anbarasan, Spectrochim. Acta A 77, 2010, 45-50.

[38]. B.J. Powell, T. Baruah, N. Bernstein, K. Brake, R.H. McKenzie, P. Meredith, M.R. Pederson, J. Chem. Phys. 120, 2004, 8608-8615.

[39]. M.A. Palafox, Int. J. Quantum Chem. 77, 2000, 661-684..

[40]. R.P. Iczkowski, J.V. Margrave, J. Am. Chem. Soc. 83, 1961, 3547-3551.

[41]. L. Larabi, Y. Harek, O. Benali, S. Ghalam, Prog. Org. Coat. 54, 2005, 256- 262.

[42]. I. Lukovits, I. Bako, A. Shaban, E. Kalman, Electrochim. Acta 43, 1998, 131-136.

[43]. R.G. Parr, L.V. Szentpaly, S.J. Liu, Am. Chem. Soc. 121, 1999, 1922- 1924.

[44]. P. Politzer, J.S. Murray, Theor. Chem. Acc. 108, 2002, 134-142.

[45]. S. Gunasekaran, R.A. Balaji, S. Kumaresan, G. Anand, S. Srinivasan, Can. J. Anal. Sci. Spectrosc. 53, 2008, 149-162.

[46]. P. Politzer, D.R. Lawrence, K. Jayasuriya, Environ. Health Perspect. 61, 1985, 191-202.